Compact Dual-band Hybrid-Fractal MIMO System for UMTS and LTE Mobile Applications

P. Prabhu and S. Malarvizhi

Department of Electronics and Communication Engineering
SRM Institute of Science and Technology, Katankulathur, Chennai, India
prabhu.beece66@gmail.com, malarvizhi.g@ktr.srmuniv.ac.in

Abstract ─ This article presents a bandwidth enriched, dual-band, compact, multiple-input-multiple-output (MIMO) antenna with high isolation for UMTS and LTE applications. The proposed coplanar waveguide (CPW)-fed, hybrid fractal MIMO antenna was created by integrating Koch fractal and Sierpinski fractal on a rectangular patch radiator. The MIMO antenna uses a rectangular shaped partial ground plane with a T-shaped stub on the ground plane to improve the isolation between radiators. The iterative technique, using the Koch curve and the Sierpinski square slot fractal was used on the rectangular patch to reduce the size of the MIMO antenna and retain the electrical performance. By using an amalgamated fractal configuration and a CPW feed, a large impedance bandwidth was achieved: 80% wide bandwidth over the operating frequency of 1.81–3.17 GHz with a compact size of 25×35 mm^2. The prototype of the optimized MIMO configuration was fabricated using the FR4 substrate, and its characteristics were measured. The proposed antenna resonates at 2.1 and 2.6 GHz. The antenna parameters, including the reflection coefficient (S11, S12, S21, and S22), surface current distributions, realized gain and radiation patterns were simulated and measured. Additionally, the diversity performances of the MIMO antenna were analyzed in terms of diversity gain (DG) and envelope correlation coefficient (ECC). The proposed antenna retains high isolation of less than -20 dB from 1.81–3.17 GHz band; the DG and the ECC are greater than 9.5 dB and less than 0.08, respectively. The peak gains of the proposed antenna are 5.8 dBi and 6.9 dBi at 2.1 GHz and 2.6 GHz, respectively. Hence, the proposed hybrid fractal MIMO antenna is a good candidate for both UMTS and LTE applications.

Index Terms ─ CPW-MIMO, Hybrid Fractal, LTE, MIMO antenna, Mobile applications, UMTS.

I. INTRODUCTION

As multiple-input-multiple-output (MIMO) antenna have improved tremendously in recent years, MIMO antenna technology is playing a vital role in modern wireless communications systems, such as in UMTS, LTE, and WLAN. The future generation of communication systems requires a heterogeneous network with an improved channel capacity and reliability for modern mobile communications standards, such as GSM, UMTS, and LTE. Therefore, multiband and broadband MIMO antenna systems are significant to current mobile handsets. MIMO antenna systems can notably improve the reliability and data rate by using the same spectrum and power level. However, in practical situations electromagnetic mutual coupling will occur among the radiators due to a limited amount of space. Hence, isolation or a new decoupling structure is essential to compact a MIMO antenna. Fractal antennas provide multi-band, broadband, and compact antenna designs for various mobile standards. The self-filling and self-affine characteristics of the fractal reduce the size of the antenna and resonate multiple frequencies with broad bandwidth. An iterative structure can be obtained by reducing the initial dimension of the fractal structure [1-5]. In addition, a Koch fractal can be used to miniaturize the antenna size and increase the electrical length [6]. The planar monopole MIMO antenna can be implemented using the hybrid fractal shape by combining the Minkowski island curve and the Koch curve fractal, operating at 1.65 GHz to 1.9 GHz [7]. Isolation and impedance of the antenna can be improved by the T-shaped strip and etching at the top of the ground plane, respectively. Two elements of a meander-line MIMO antenna proposed that operates at 699–798 MHz and 1920–2170 MHz for PCS and LTE, respectively [8]. The polarization diversity method can be utilized to decouple the two antenna elements. By stimulating orthogonal polarization between the two antenna elements, polarization diversity can be achieved [9, 10]. In [11, 12], high isolation can be obtained by attaching parasitic elements to the ground plane. Isolation between the two elements can be enhanced and achieved through the use of a metal strip and two bent slits [13]. To enhance the port to-port isolation, a protruded ground may be utilized [14]. Dual orthogonal polarization and parasitic elements may be employed for cavity-backed bow tie MIMO

Submitted On: July 25, 2017
Accepted On: December 24, 2018

antenna [15]. The MIMO antenna can be implemented through the use of circular and annular slots, and a varactor diode may be used inside its annular slot to make it re-configurable [16-18]. Although many MIMO antennas have been implemented in the past decade, there is a need for high isolation with a high degree of miniaturization [18]. Fractal configuration, having space-filling and self-affine properties, can create a significant electrical length in a small space. Hence, this article proposes the CPW-fed composite fractal MIMO system with high isolation for modern mobile applications. This hybrid fractal antenna was created through the amalgamation of the Koch fractal and Sierpinski fractal with a miniaturized size of 25×35 mm^2. The antenna consists of two square-shaped hybrid fractal radiators and a T-shaped stub, which is connected to the ground to enhance isolation between the ports. Comparison of existing MIMO antenna parameter with proposed hybrid fractal MIMO antenna is shown in Table 1.

Table 1: Comparison of existing MIMO antenna parameter with proposed hybrid fractal MIMO antenna

Ref.	Size (mm)	Operating Bands (GHz)	Isolation (dB)	Peak Gain (dBi)
[7]	100×50	1.65-6.25	-15	2.5-7.8
[8]	80 X 67	0.699-2.17	-22	5
[9]	50 X 26	2.45	-30	-
[10]	120 X 140	2.4 & 2.6	-15	5.5-6.4
[12]	50 X 100	1.79-3.77	-20	2-6
[13]	78 X 40	2.4-6.55	-18	-
[16]	60 X 120	1.8-2.45	-15	2.43
Pro	25 X 35	2.1 & 2.6	< -20	7

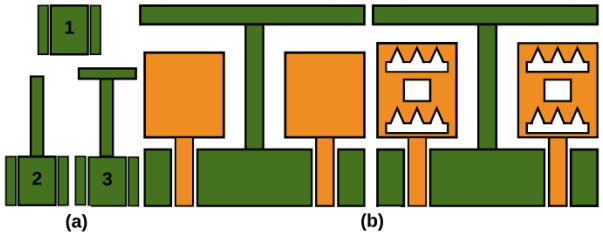

Fig. 1. (a) Development of decoupling structure, and (b) 0_{th} and 1_{st} iteration structure of proposed hybrid fractal MIMO system.

II. ANTENNA DESIGN PROCEDURE

A. Fractal Iterative Function System (IFS)

The Iterative Function System (IFS) is a very convenient technique for correctly generating various fractal configurations. The utilization of the affine transform sequence (v) is an essential character of IFS [3]. The regeneration (v) is expressed as:

$$\begin{pmatrix} x \\ y \end{pmatrix} = \begin{pmatrix} p & q \\ r & s \end{pmatrix} \begin{pmatrix} v \\ w \end{pmatrix} + \begin{pmatrix} t \\ u \end{pmatrix}, \quad (1)$$

$$v(x,y) = (px+qy+s, rx+dy+u). \quad (2)$$

Where, p, q, r, s, t and u are real coefficients.

On the other hand, the movement of fractal elements in the space based on these elements is a scaling factor, are rotation factors, by θ_1, θ_2 and linear rendering it can be represented as $p = \delta_1 \cos\varphi_1, s = \delta_2 \cos\varphi_2$. Consider v_1, v_2...,v_N as a collection of successive transmutations, and the fundamental structure is B. By using the collection of transformations to the primary structure geometry, a new configuration is formed. In addition to that, accumulating the results from v_1(B), v_2(B),...,v_N(B), it can be exposed as $q = \delta_1 \sin\varphi_1$, $r = \delta_2 \sin\varphi_{2x}$ and $V_1(B) = \bigcup_{n=1}^{N} v_n(B)$ where 'V' is the Hutchinson vector. The fractal configuration is achieved by reusing the previous configuration. Using a fractal calculation, a Sierpinski carpet and Koch fractals were obtained.

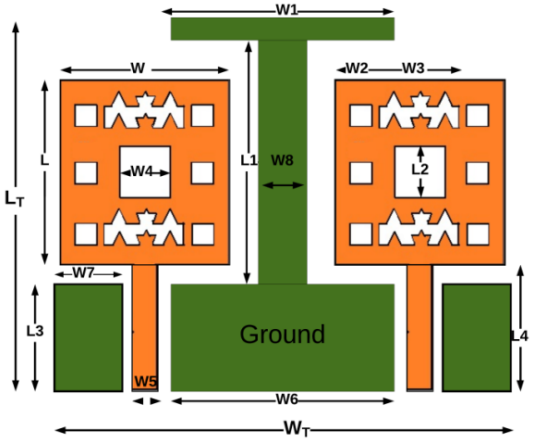

Fig. 2. Geometry of proposed second iteration hybrid fractal MIMO system.

B. Koch and Sierpinski fractal formation

The Koch fractal configuration is determined by applying the formulas [3, 4]. The IFS of Sierpinski fractal and Koch fractal are as shown below,

$$W_q \begin{pmatrix} x \\ y \end{pmatrix} = \begin{pmatrix} \delta_{q1}\cos\theta_{q1} & -\delta_{q_2}\sin\theta_{q2} \\ \delta_{q1}\sin\theta_{q1} & \delta_{q_2}\cos\theta_{q2} \end{pmatrix} \begin{pmatrix} x \\ y \end{pmatrix} + \begin{pmatrix} t_{q1} \\ t_{q2} \end{pmatrix}. \quad (3)$$

The Scaling operator of Koch fractal is shown below, θ_q- the angle of slope between the two-part of the initiators. $\theta_{qi}=60^0$and t_{q1} are the movements of the parts on the correlative surface.

Sierpinski fractal geometry can also be obtained using fractal IFS. The calculation method is shown below,

$$v_1(x,y)=\left[\frac{1}{3}x;\frac{1}{3}y\right], v_2(x,y)=\left[\frac{1}{3}x;\frac{1}{3}y+\frac{1}{3}\right], \quad (4)$$

$$v_3(x,y)=\left[\frac{1}{3}x;\frac{1}{3}y+\frac{2}{3}\right], \; v_4(x,y)=\left[\frac{1}{3}x+\frac{1}{3}y;\frac{1}{3}y\right], \quad (5)$$

$$v_5(x,y)=\left[\frac{1}{3}x+\frac{1}{3};\frac{1}{3}y+\frac{2}{3}\right], v_6(x,y)=\left[\frac{1}{3}x+\frac{1}{3};\frac{1}{3}y\right], \quad (6)$$

$$v_7(x,y)=\left[\frac{1}{3}x+\frac{2}{3};\frac{1}{3}y+\frac{1}{3}\right], v_8(x,y)=\left[\frac{1}{3}x+\frac{2}{3};\frac{1}{3}y+\frac{1}{3}\right]. \quad (7)$$

Table 2: Iteration computation of fractal (for 2 iterations)

Level	Length (In Terms of Fraction)	Boundary	Area (mm^2)
Initial square	1	(4). (1) = 4	$(1)^2 = 1$
1st iteration	1/2	(4).(1/2) = (4/2) = 2	$(1/2)^2 = 1/4$
2nd iteration	1/4	(4). (1/4)=1	$(1/4)^2 = /16$

III. ANTENNA STRUCTURE

Figure 1 (a) development of decoupling structure, zeroth and Fig.1 (b) illustrates the first iteration structure of the proposed antenna, whereas Fig. 2 depicts the configuration of the proposed hybrid fractal MIMO antenna. The suggested MIMO system is printed on a FR4 mater substrate with a thickness of 1.6 mm and dielectric constant of 4.4. The objective of using a hybrid fractal configuration is the development of the characteristic of space-filling, in which the structure converts into the reduced dimension of the antenna with multi-band features. The proposed rectangular patch configuration consists of a pair of fractals, such as a Sierpinski carpet and a Koch fractal. Furthermore, the rectangular patch antenna results in improved performance [5].

The iteration techniques were used in the rectangle shaped antenna to achieve the three repetitions for the Koch and Sierpinski fractals. The 0-th iteration is the fundamental configuration of the suggested antenna, consisting of a rectangular patch radiator with two rectangular ground planes, a CPW feed, and a small current flowing in the middle of the rectangular patch. The first iteration of the Sierpinski fractal configuration was created through the insertion of square slots in the center of a rectangular radiator. Since there is negligible current in the center, this does not change the performance characteristics of the antenna. Subsequently, by contracting the rectangular slot of the first iteration at a ratio of 0.33, a second iteration pattern was achieved and cut out, comprising the central square shaped slot of the first repetition structure. Similarly, the three iterations of the Koch curve fractal were achieved using the IFS method. The 0-th iteration consists of a rectangular-shaped radiator with rectangular slots at its upper and lower part. The first iteration was obtained by splitting a small rectangular slot into three parts. The length of the triangular slot formed in the center had a slope of 60^o between the two parts. The second iteration of the Koch fractal was achieved by reproducing the same method as the first iteration. The numerical calculation of fractal iterations up to 2 iterations are shown in Table 2. Since fractals have various patterns such as squares and triangles, the surface current of the radiator increased. Consequently, multiple frequencies resonate without altering the dimension of the antenna. The antenna was triggered by CPW feed with partial rectangular ground plane. CPW feed technology was utilized because of its advantages, including its wide bandwidth, easy fabrication, and other beneficial properties, such as the absence of loss. The antenna consists of two rectangular-shaped partial ground planes which produce a capacitive effect by canceling the inductive effect of a square radiator and provide purely resistive impedance to antenna configuration. Multiple resonance frequencies and enhanced bandwidth coverage can be achieved through the successive optimization strategies: increasing the number of fractal repetitions, regulating the width of the rectangular-shaped patch and the height of the two grounds surface. The optimized geometry of the proposed MIMO system is presented in Table 3.

Table 3: Geometry of proposed hybrid fractal MIMO antenna dimensions (all dimensions are in mm)

W_T	W	W_1	W_2	W_3	W_4	W_5	W_6	W_7	W_8
35	13	10	1	6	3	3	20	6	4
L_T	L	L_1	L_2	L_3	L_4				
25	11	19	3	4.5	4.5				

Using a decoupling structure reduces mutual coupling, but the problem with this approach is that a MIMO structure occupies considerable space. The design put forward in this work features a T-shaped stub decoupling structure, which effectively reduces the mutual coupling of radiators. Figure 1 (a) shows the development of the decoupling structure. MIMO antenna 1 is a compact device at 4.5×35 mm^2 and represents a combination of two hybrid fractals that share the same ground plane. Because of the diminutive size of the antenna, the partial ground plane acts as a radiating element and radiates energy normal to the radiating element. Due to the current distribution on the ground plane, there is influential coupling between the two MIMO system elements. Therefore, the isolation of MIMO antenna 1 is poor, as shown in Fig. 4 (a).

In MIMO antenna 2, the attachment of a rectangular-shaped stub to the ground plane changes the surface current on the partial ground, thereby improving isolation. That is, S12 / S21 is < - 15 dB at 2 to 10 GHz.

As shown in Fig. 4 (a), however, isolation is needed for improvement at resonating frequencies. The size of the T-shaped stub was optimized to improve isolation. The results are shown in Fig. 4 (a). In MIMO antenna 3, a rectangular stub is connected horizontally with a vertical stub that is attached to the ground plane, thus enhancing isolation in the operating frequencies. That is, S12 / S21 less than < - 20 dB at 1 to 10 GHz. In order to demonstrate the performance of the suggested isolation configuration, the surface current of the antenna at different frequencies is shown in Figs. 5 (a)-(d).

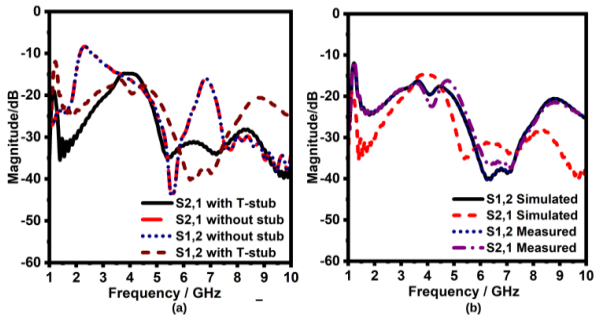

Fig. 4. (a) Simulated S12/S21 -parameters for the various decoupling structures. (b) Simulated and measured S12/ S21-parameters of proposed MIMO antenna with T-Stub decoupling structures.

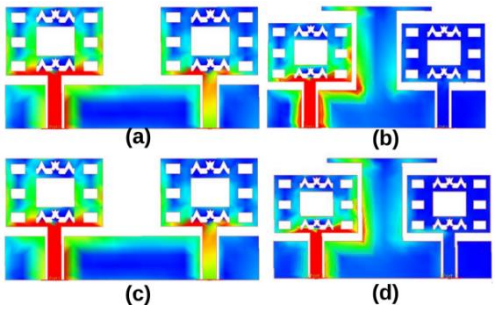

Fig. 5. Surface current of the hybrid fractal MIMO system with and without an isolation structure with port 1 (energized) (a) 2.1 GHz, (b) 2.6 GHz, (c) and (d).

The surface current distributions of two resonant frequencies were obtained. Without the stub isolation structure, energizing port 1 causes a strong current to be coupled at port 2. With the T-stub isolation structure, energizing port 1 causes no coupling current at port 2, and energizing port 2 causes no coupling current at port1. Therefore, the coupling current from ports 1 to 2 and vice versa is suppressed by the T-shaped stub decoupling structure proposed in the partial ground plane. In order to verify the effectiveness of the proposed MIMO system, a simulation was carried out using Microwave Studio and Advanced Design System (ADS).

IV. RESULTS AND DISCUSSIONS

The proposed MIMO antenna was printed on the FR4 substrate, after which the prototype was measured using Keysight N9926A vector network analyzer to verify the simulation results. Figure 8 shows the fabricated antenna with a CPW feed. Three hybrid fractal iterations were designed for the proposed MIMO antenna, and because the second iteration has fractals of various shapes, performance improves over that observed under all other iterations. Also, the current distribution occurs maximum at the corners of the fractals. The simulated S-parameter for the different iterations (e.g., zeroth, first, second iterations) is depicted in Fig. 6. It can be perceived from Fig. 6, that the second iteration has better performance compared to other iterations. The correlation of the simulated results for various partial ground sizes is presented in Fig. 7. Resonance is achieved at 2.1 and 2.6 GHz. Besides, the second iteration of a composite fractal configuration with a partial ground plane having the size of 35×4.5 mm^2 was fabricated on FR4 substrate presents the optimal design. The simulated and measured reflection coefficient (S11) of the proposed hybrid fractal MIMO system for optimized dimensions are shown in Fig. 8. The simulation and measured bandwidth of the proposed MIMO antenna is 2 GHz (1.9–3 GHz). MIMO antennas that resonate at 2.1 GHz (UMTS) and 2.62 GHz (LTE) have reflection of –48 and –47 dB, respectively. This is according to the results mentioned in [7].

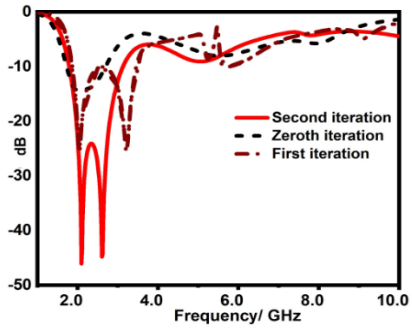

Fig. 6. Simulated Return Loss of Hybrid Fractal for Zeroth Iteration, First Iteration, and Second Iteration.

The comparison of simulated and measured S12/ S21 parameters of the proposed MIMO antenna with T-stub isolation configuration is shown in Fig. 4 (b). From the figure, it can be observed that the isolation between two radiators in the proposed MIMO system is less than –20 dB over the operating frequency band. It can be inferred from these results that the simulated and measured insertion loss are approximately the same, implying the fact that it is suitable for MIMO systems. The radiation aspects of the proposed composite fractal MIMO antenna system were also investigated. The

composite structure of Koch's and Sierpinski fractal increases surface current distribution uniformly throughout the rectangular patch and creates a radiation pattern. Besides, CPW feed employed with two partial ground planes that contributed to obtain better radiation characteristics.

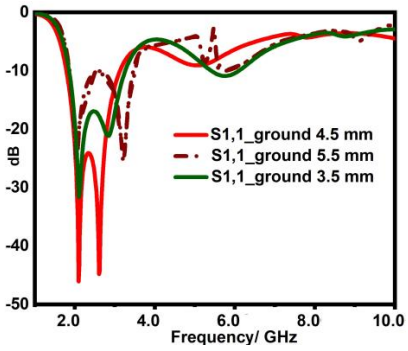

Fig. 7. Simulated reflection coefficient of hybrid fractal MIMO antenna with different ground size.

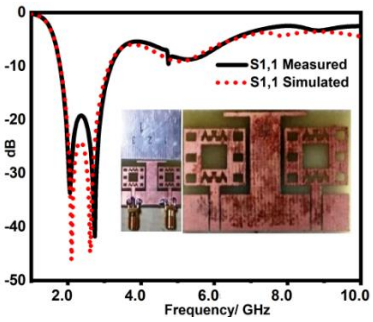

Fig. 8. Simulation and Measured S11 for the Proposed Hybrid Fractal MIMO System.

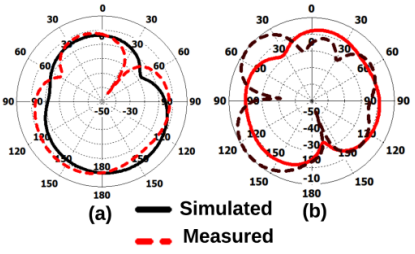

Fig. 9. Simulated and Measured Radiation Pattern of the proposed MIMO System at 2.1 and 2.6 GHz

The simulated and measured radiation patterns for the proposed antenna in the x-y plane at 2.1and 2.6 GHz are illustrated in Figs. 9 (a) and (b). From Figs. 9 (a) and (b), it can be perceived that the radiation pattern is approximately constant at the operating frequency band and the composite fractal MIMO antenna radiates uniformly in all directions. The peak gain of the MIMO antenna is 5.8 and 6.9 dBi at 2.1 and 2.6 GHz, respectively. The antenna's efficiency levels were 85% and 90% at 2.1 and 2.6 GHz, respectively. Therefore, the proposed MIMO structure is better in terms of size, peak gain, isolation, ECC and DG when compared to existing MIMO antennas mentioned Table 1. Hence, it is well suited for UMTS and LTE applications.

V. MIMO PERFORMANCE

The MIMO characteristics of the proposed antenna are assessed by diversity gain (DG) and envelope correlation coefficient (ECC). Isolation between radiating components can be investigated from the perspective of ECC. ECC can be determined using either the scattering parameter method or the fair field radiation pattern. The scattering parameters based ECC calculation is preferred because 3D far field measurement is difficult. The ECC of the MIMO antenna system is calculated by the following equation [4],

$$ECC = \frac{\left|S_{11}^{*}S_{12} + S_{21}^{*}S_{22}\right|^{2}}{\left(1-\left|S_{11}\right|^{2}-\left|S_{21}\right|^{2}\right)\left(1-\left|S_{22}\right|^{2}-\left|S_{12}\right|^{2}\right)}. \quad (8)$$

The diversity gain of the MIMO antenna system is evaluated using following equation $DG = 10\sqrt{1-ECC^{2}}$. Although the ECC ideally must be zero, the practical limit of ECC is less than 0.5 for an isolated MIMO diversity antenna. The ECC of the recommended composite fractal MIMO antenna is estimated using both S-parameter and radiation pattern method that is less than 0.08. It is perceived from Fig. 10. The DG of the proposed hybrid fractal MIMO antenna system can be observed in Fig. 10 that shows the simulated and measured DG that is greater than 9.5 dB.

VI. CONCLUSION

We have proposed a bandwidth-enriched, dual-band, compact MIMO antenna with high isolation for UMTS and LTE applications. By using an amalgamated fractal configuration and CPW feed, a broad impedance bandwidth of 80% is obtained at 1.81 to 3.17 GHz with a miniature size of 25×35mm^2 . The proposed hybrid fractal MIMO antenna provides good impedance matching over the 1.81 to 3.17 GHz frequency band. With the help of the T-shaped stub isolation configuration, isolation between ports is enhanced; that is, less than −20 dB is attained throughout the operating frequency band. The proposed hybrid fractal MIMO system is also a right candidate for MIMO multi-polarized performance as the DG, and the ECC is greater than 9.5 dB and less than 0.08, respectively, throughout the operating band. The obtained peak gains of the proposed antenna are 5.8 and 6.9 dBi at 2.1GHz and 2.6 GHz, respectively. The composite fractal MIMO antenna has omnidirectional radiation pattern at 2.1 and 2.6 GHz. The simulation and measurement results show that the proposed MIMO

structure is better in terms of size, peak gain, isolation, ECC and DG when compared to existing MIMO antennas. Hence, the suggested hybrid fractal MIMO antenna system is well suited for UMTS and LTE applications.

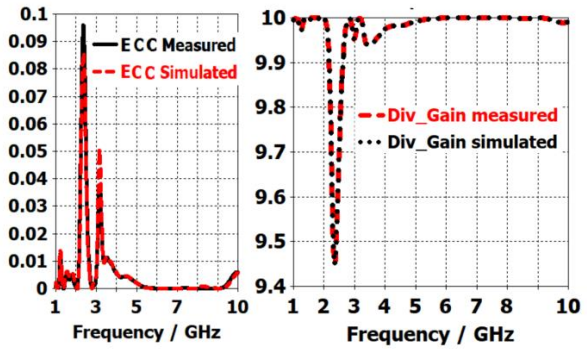

Fig. 10. Simulated and measured ECC and DG for proposed MIMO antenna.

REFERENCES

[1] B. B. Mandelbrot, "The fractal geometry of nature," *American Journal of Physi*cs, vol. 51, no. 3, p. 286, 1983.

[2] D. H. Werner and R. Mittra, *Frontiers in Electromagnetics*. New York: Wiley, 1999.

[3] K. Falconer, *Fractal Geometry: Mathematical Foundation and Application*. New York, NY, USA: Wiley, 1990.

[4] H. Peitgen, H. Jurgens, and D. Saupe, *Chaos and Fractals: New Frontiers of Science*. Berlin, Germany: Springer-Verlag, 1992.

[5] D. H. Werner and S. Ganguly, "An overview of fractal antenna engineering research," *IEEE Antennas Propag. Mag.*, vol. 45, no. 1, pp. 38-57, 2003.

[6] C. P. Baliarda, J. Romeu, and A. Cardama, "The Koch monopole: A small fractal antenna," *IEEE Trans. Antennas Propag.*, vol. 48, pp. 1773-1781, 2000.

[7] Y. K. Choukiker, S. K. Sharma, and S. K. Behera, "Hybrid fractal shape planar monopole antenna covering multiband wireless communications with MIMO implementation for handheld mobile devices," *IEEE Transactions on Antennas and Propagation*, vol. 62, no. 1, pp. 12-13,2014.

[8] M. M. Morsy and A. M. Morsy, "Dual-band meander-line MIMO antenna with high diversity for LTE/UMTS router," *IET Microwaves, Antennas Propagation*, vol. 12, no. 3, pp. 395-399, 2018.

[9] M. M. Morsy, "2.45GHz dual polarized aperture-coupled antennas with high isolation performance," in *Proceedings of the 2012 IEEE International Symposium on Antennas and Propagation*, pp. 1-2, July 2012.

[10] A. MoradiKordalivand, T. A. Rahman, and M. Khalily, "Common elements wideband MIMO antenna system for WiFi/LTE access-point Applications," *IEEE Antennas Wireless Propag. Lett.*, vol. 2014, pp. 13-1601, 2014.

[11] Y. Wang and Z. Du, "A printed dual-antenna system operating in the 2.4-GHz WLAN bands for mobile terminals," *IEEE Antennas and Wireless Propagation Letters*, vol. 13, pp. 233-236, 2014.

[12] A. Toktas and A. Akdagli, "Wideband MIMO antenna with enhanced isolation for LTE, WiMAX and WLAN mobile handsets," *Electronics Letters*, vol. 50, no. 10, pp. 723-724, May 2014.

[13] J.-F. Li, Q.-X. Chu, and T.-G. Huang, "A compact wideband MIMO antenna with two novel bent slits," *IEEE Transactions on Antennas and Propagation*, vol. 60, no. 2, pp. 482-489, Feb 2012.

[14] J.-F. Li, Q.-X. Chu, Z.-H. Li, and X.-X. Xia, "Compact dual band-notched UWB MIMO antenna with high isolation," *IEEE Transactions on Antennas and Propagation*, vol. 61, no. 9, pp. 4759-4766, Sept. 2013.

[15] H.-T. Hu, F.-C. Chen, and Q.-X. Chu, "A wideband U-shaped slot antenna and its application in MIMO terminals," *IEEE Antennas and Wireless Propagation Letters*, vol. 15, pp. 508-511, 2016.

[16] R. Hussain, G. Asim, and M. S. Sharawi, "Annular slot-based miniaturized frequency-agile MIMO antenna system," *IEEE Antennas and Wireless Propagation Letters*, vol. 16, pp. 2489-2492, 2017.

[17] T. Shabbir, R. Saleem, M. F. Shafique, and A. Akram, "UWB-MIMO qauadruple with FSS inspired decoupling structures and defected grounds," *The Applied Computational Electromagnetic Society*, vol. 30, no. 2, pp. 184-190, 2015.

[18] J. Mazloum and N. Ojaroudi, "Utilization of protruded strip resonators to design a compact UWB antenna with WiMAX and WLAN notch bands," *The Applied Computational Electromagnetic Society*, vol. 31, no. 2, pp. 12-13, 2016.